JJMIE

Volume 3, Number 2, June. 2009
ISSN 1995-6665
Pages 97 - 104

Jordan Journal of Mechanical and Industrial Engineering

Strain-Concentration Factor of Cylindrical Bars with Double Circumferential U-Notches under Static Tension

Hitham M. Tlilan*, Ali M. Jawarneh, Ahmad S. Al-Shyyab

Department of Mechanical Engineering, Faculty of Engineering, The Hashemite University
P.O. Box 150459, Zarqa 13115, Jordan

Abstract

The interference effect on the new strain concentration factor (SNCF), which has been defined under triaxial stress state; is studied using the Finite Element Method (FEM).To this end, cylindrical bars with double circumferentially U-notches under static tension are employed. he new SNCF is constant in the elastic deformation and the range of this constant value increases with increasing notch pitch (lo) in the range 0.0 <lo≤ 0.5 mm, then it decreases with increasing lo, and reaches a value nearly equal to that of the single circumferential U-notch. This becomes prominent with decreasing notch radius. As plastic deformation develops from the notch root; the new SNCF increases from its elastic value to a maximum value. On further plastic deformation, the new SNCF decreases with plastic deformation. The current results indicate that the notch pitch, where the interference effect is more pronounced on the new SNCF, is $0.0 \le l_o \le 5$ mm.

Keywords: Finite Element Method; Interference Effect, Notch; Tension; Strain-Concentration Factor

Nomenclature

A	net-section area
d_o	initial net-section diameter
D_o	initial gross diameter
E	Young's modulus
K_ε^{con}	conventional strain-concentration factor
K_ε^{new}	new strain-concentration factor
P	tensile load
P_Y	tensile load at yielding at the notch root
r	current distance from the center of the net-section ($0 \le r \le r_n$)
r_n	current net-section radius = $d/2$
s	$= r/r_n$ ($0 \le s \le 1.0$)
$2\ln(d_o / d)$	deformation parameter
$[2\ln(d_o / d)]_Y$	deformation parameter at yielding at notch root
η	the ratio of deformation parameter to that at yielding at the notch root $= \dfrac{2\ln(d_o / d)}{[2\ln(d_o / d)]_Y}$
ε_z	axial strain
$(\varepsilon_z)_{av}^{con}$	conventional average axial strain
$(\varepsilon_z)_{av}^{new}$	new average axial strain
$(\varepsilon_z)_{max}$	maximum axial strain
ν	Poisson's ratio
ρ_o	initial notch radius
σ_{eq}	equivalent stress
equivalent stress	$= \left\{(\sigma_z-\sigma_\theta)^2+(\sigma_\theta-\sigma_r)^2+(\sigma_r-\sigma_z)^2\right\}^{1/2} / \sqrt{2}$
$(\sigma_{eq})_{max}$	equivalent stress at the notch root
σ_r , σ_z , σ_θ	radial , axial and tangential stresses
σ_Y	yield stress
$(\sigma_z)_{av}$	average axial stress at the net section = P/A
$(\sigma_z)_{max}$	axial stress at the notch root in elastic deformation
$(\sigma_\theta)_{max}$	tangential stress at the notch root in elastic deformation

* Corresponding author. hitham@hu.edu.jo.

Abbreviations

SNCF	strain concentration factor
SSCF	stress concentration factor

1. Introduction

Stress and strain concentrations in any type of loading arise when uniformity of geometry is disrupted. Particularly, geometrical irregularities such as notches, grooves, holes, or defects are acting as local stress and strain raisers. They alter the lines of the principal stress; and bring about the stress and strain concentrations at the notch tip. Moreover, biaxial or triaxial stress state is produced at the net section even if the single loading, like axial tension, is applied to the notched bars. This single loading generates the uniaxial stress state in the unnotched part with the gross section. It should be noted that the net section is subjected simultaneously to the stress and strain concentrations and the multiaxial stress state.

Many numerical analyses and theoretical studies have been conducted to obtain the elastic stress-concentration factor (SSCF); the results have been published and used for engineering design [1- 6]. The Neuber's approximate analytical solutions are the main source, concerning the notch depth effect on the elastic SSCF [3-7]. Neuber's rule predicts that the plastic SNCF increases, and the plastic SSCF decreases from their elastic values as plastic deformation develops from the notch root [7]. Many experimental or analytical studies under static axial tension have confirmed this prediction [7-13]. These results indicate that the SNCF is more important than the SSCF [14-15]. This is because the plastic SNCF maintains a value much greater than unity while the plastic SSCF decreases towards unity.

There have been many studies used to calculate the stress and strain at the notch root under static and cyclic tensile loading using Neuber's rule [13, 16-21], Glinka's method [18-19, 21-22], and linear rule [13, 17, 19, 23]. The predicted values have been compared with finite element and experimental ones. The results of these comparisons indicate that there is no rule which can accurately predict the magnitude of the axial strain at the notch root. Particularly, in notched rectangular bars, the accuracy of the prediction decreases with increasing thickness. This is because the conventional strain-concentration factor (= maximum axial strain/average or nominal strain) is defined under uniaxial stress state while axial strain at the notch root occurs under triaxial stress state [14, 15]. Strain-concentration factor should thus be defined under triaxial stress state at the net section [14-15].

A new SNCF has been proposed under the axial tension [14]. This new SNCF has been defined under triaxial stress state at the net section. This has enabled new SNCF to provide reasonable values consistent with the concave distributions of the axial strain on the net section [14-15].

Moreover, this new SNCF has removed the contradiction in conventional SNCF having values less than unity in spite of the concave distributions of the axial strain under elastic-plastic deformation. The nominal strain of the conventional SNCF, as described above, has been defined under the uniaxial stress state. The uniaxial stress state is completely different from the stress state at the net section, namely, the triaxial stress state [14-15]. This causes the above contradiction of the conventional SNCF. This means that the SNCF for any type of loading must therefore be defined under the triaxial stress state at the net section. This is because the axial strain at the notch root occurs under the triaxial stress state.

The effect of notch depth on the SNCF and SSCF under static tension and under pure bending has been studied by [15,24,25-26].

The specimens employed are circumferentially U-notch cylindrical bars for static tension and rectangular bars with single-edge U-notch for pure bending. The results indicate that the new SNCF is more reasonable than the conventional SNCF and SSCF. Therefore, this newly defined SNCF must be applied to different types of notches or geometries and different types of loading.

Some studies examined the interference effect on the elastic SSCF of the flat bars with double U- or semicircular notches under tension. The obtained relations between the elastic SSCF and the notch pitch have been published and used for engineering design [3]. These studies show that SSCF subjected to interference effect is less than the SSCF of a single notch. Few studies have been carried out on the interference effect on the elastic SSCF of cylindrical bars with double U- or semicircular notches under tension. Moreover, only two studies have been performed on the interference effect on strength such as yield point load, ultimate tensile strength, and deformation properties of notched bars under tension [27-28]. In these studies, the interference effect has also been discussed on the elastic SSCF of cylindrical bars with double U-notches under tension.

Unfortunately, the interference effect on elastic and elastic-plastic new SNCF has not been evaluated. In this paper, the cylindrical bar double circumferential U-notches is employed to study the interference effect on the elastic-plastic new SNCF.

2. Strain-Concentration Factor under Static Tension

For tensile loading, the new strain-concentration factor (SNCF) has been defined as the ratio of the maximum axial strain at the notch root $(\varepsilon_z)_{max}$ to the new average axial or new nominal strain $(\varepsilon_z)_{av}^{new}$[14] .

$$K_{\varepsilon}^{new} = \frac{(\varepsilon_z)_{max}}{(\varepsilon_z)_{av}^{new}} \quad (1)$$

Since the maximum axial strain at the notch root is independent of definition, then the new SNCF is introduced by a new definition of the average axial strain $(\varepsilon_z)_{av}^{new}$. For circumferentially notched cylindrical bars $(\varepsilon_z)_{av}^{new}$ is defined as follows [14]:

$$(\varepsilon_z)_{av}^{new} = \frac{1}{\pi r_n^2}\int_0^{r_n} \varepsilon_z(r)\, 2\pi\, r\, dr = 2\int_0^1 \varepsilon_z(s)\, s\, ds \quad (2)$$

where $s = r/r_n$. In the elastic level of deformation, $(\varepsilon_z)_{av}^{new}$ can be transformed into the following equation:

$$\begin{aligned}(\varepsilon z)_{av}^{new} &= \frac{1}{\pi r_n^2}\int_0^{r_n}\left[\frac{\sigma_z}{E}-\frac{\nu}{E}(\sigma_\theta+\sigma_r)\right]2\pi\, r\, dr \\ &= \frac{1}{E}\cdot\frac{1}{\pi r_n^2}\int_0^{r_n}\sigma_z\, 2\pi\, r\, dr-\frac{\nu}{E}\cdot\frac{1}{\pi r_n^2}\int_0^{r_n}(\sigma_\theta+\sigma_r)\,2\pi\, r\, dr \\ &= \frac{1}{E}\cdot\frac{P}{\pi r_n^2}-\frac{\nu}{E}\cdot\frac{1}{\pi r_n^2}\int_0^{r_n}(\sigma_\theta+\sigma_r)\,2\pi\, r\, dr \\ &= \frac{(\sigma z)_{av}}{E}-\frac{\nu}{E}\cdot\frac{1}{\pi r_n^2}\int_0^{r_n}(\sigma_\theta+\sigma_r)\,2\pi\, r\, dr\end{aligned} \quad (3)$$

Where E and ν are the Young's modulus and Poisson's ratio, respectively. Equation (3) can be rewritten as follows:

$$(\varepsilon_z)_{av}^{new} = \frac{(\sigma_z)_{av}}{E}-\frac{2\nu}{E}\int_0^1\{\sigma_\theta(s)+\sigma_r(s)\}\, s\, ds \quad (4)$$

This equation indicates that $(\varepsilon_z)_{av}^{new}$ is defined under the triaxial stress state at the net section.

It should be noted that $(\varepsilon_z)_{av}^{new}$, given by Eq. (2), is defined under the triaxial stress state also in plastically deformed area at the net section.

This is because of the fact that plastic component of the axial strain is directly related to the triaxial stress state, as is indicated by the theory of plasticity. Since the plastic deformation develops from the notch root; i.e. $\sigma_{eq} > \sigma_Y$, the newly defined average axial strain has been calculated using the incremental or flow theory, which relates the stresses to the plastic strain increments. In the plastic deformation, the strains in general are not uniquely determined by the stresses but depend on the entire history of loading. The definition under the triaxial stress state gives reasonable results consistent with the concave distribution of the axial strain at any deformation level [14-15, 24-25].

The conventional SNCF under static tension has been defined as follows

$$K_\varepsilon^{con} = \frac{(\varepsilon_z)_{max}}{(\varepsilon_z)_{av}^{con}} \quad (5)$$

Where $(\varepsilon_z)_{max}$ is the maximum axial strain at the notch root and $(\varepsilon_z)_{av}^{con}$ is the conventional average axial strain. This conventional SNCF has been defined under uniaxial stress state at the net section. This is because the conventional average axial strain $(\varepsilon_z)_{av}^{con}$ has been defined under uniaxial stress state [13-14]. In elastic deformation, the axial stress σ_z at the notch root $(\sigma_z)_{max}$ is much greater than $(\sigma_z)_{av}$, and the equivalent stress at the notch root $(\sigma_{eq})_{max}$ is a little lower than $(\sigma_z)_{max}$ under the biaxial tensile stress state. This indicates that the small plastic deformation occurs around the notch root even in the range $(\sigma_z)_{av} \le \sigma_Y$ when $(\sigma_z)_{av}$ approaches σ_Y. Even in this range $(\varepsilon_z)_{av}^{con}$ is given by

$$(\varepsilon_z)_{av}^{con} = \frac{(\sigma_z)_{av}}{E} \quad (6)$$

This equation indicates that the conventional definition has neglected the effect of tangential σ_θ and radial stresses σ_r. On further development of plastic deformation, i.e. in the range $(\sigma_z)_{av} > \sigma_Y$, $(\varepsilon_z)_{av}^{con}$ is determined using the uniaxial true stress–total strain curve $\sigma = f(\varepsilon)$. The reason for using this curve is that $(\varepsilon_z)_{av}^{con}$ is defined under the uniaxial stress state, and $(\sigma_z)_{av}$ is based on the instantaneous area of the net section. The conventional average axial strain is therefore given by

$$(\varepsilon_z)_{av}^{con} = f^{-1}\{(\sigma_z)_{av}\} \quad (7)$$

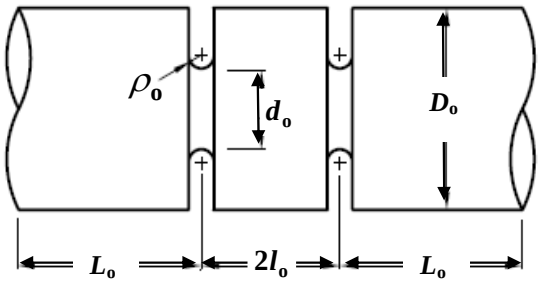

Figure 1. Specimen geometries.

3. Specimen Geometries

The employed cylindrical bar with double circumferential U-notches is shown in Fig.1. The net-section diameter d_o of 3.34 mm, and the gross diameter D_o of 16.7 mm were selected to give the net-to-gross diameter ratio d_o/D_o of 0.2. Figure 1 shows that the specimen length is expressed as $(2L_o+2l_o)$, where $2L_o$ is the unnotched length from the notch center to the loaded end, and $2l_o$ is the notch pitch or the distance between the centers of the two notches. The unnotched length is held constant, while the half notch pitch l_o is varied from 0.0 to 25 mm to examine the interference effect of the double circumferential U-notches. It should be noted that the notch pitch l_o= 0.0 mm represents the cylindrical bar with a circumferential U-notch, perpendicular to the axial direction. Two notch radii ρ_o of 0.5 and 2.0 mm are employed to vary the notch sharpness $d_o/2\rho_o$.

4. Finite Element Mesh for Double Circumferential U-Notches

Figure 2 shows a finite element mesh of one quarter of a notched specimen with double circumferential U-notches. An eight-node axisymmetric isoparametric quadrilateral ring element, with biquadratic interpolation and full integration - type 28 in MARC classifications, is

employed. This type of element uses the nine integration points, i.e. Gauss points.

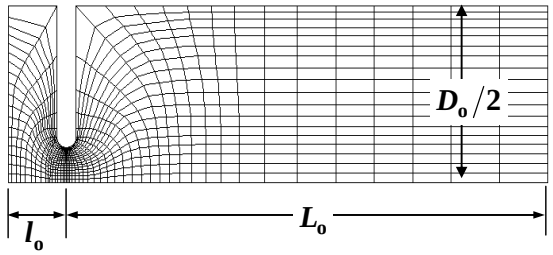

Figure 2. Finite element model.

The FEM calculations were performed under the axisymmetric deformation. This deformation was given under the condition that the axial displacement at the gross section in the center of the notch pitch and the radial displacement at the central axis are zero. The increments of the axial displacement were applied at the right end of the unnotched part. The magnitude of the increment was small enough to provide an elastic solution for the first few increments in each notched specimen.

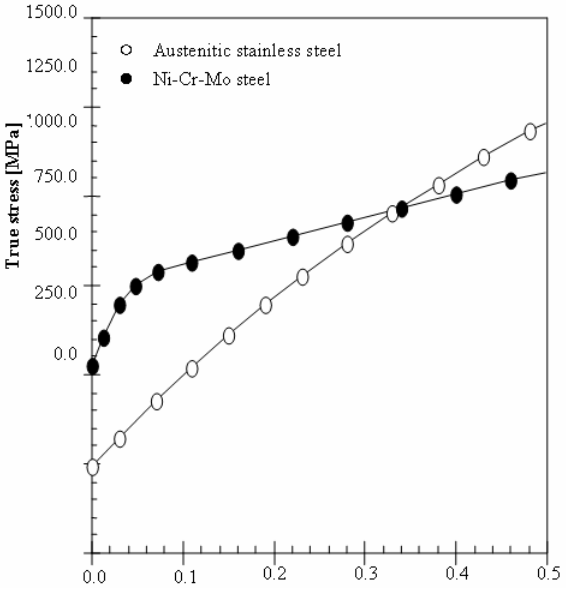

Figure 3. True stress – plastic strain curves.

All of the current calculations were carried out using MSC. Marc software. In elastic deformation, the stress-strain relationship is linear while it is nonlinear in plastic deformation. The program was developed on the basis of displacement method. After the start of plastic deformation, the nonlinear relations are used, and hence equations should be solved incrementally. Iterations are performed within each increment to satisfy the equilibrium and convergence at the end of each stage. In order to ensure the accuracy of the results and their independence with respect to the number of nodes used in the discretization process, several meshes were tested. A grid independent solution study was made by performing the simulations for different meshes.

5. Material Properties

The materials employed are an Austenitic stainless steel and an Ni-Cr-Mo steel. Young's modulus E, Poisson's ratio ν and the tensile yield stress σ_Y are listed in Table 1. The true stress-plastic strain curves were obtained from tension tests. In order to express the stress-strain curve accurately, the obtained relation was divided into a few ranges of plastic strain, and in each range the following fifth-degree polynomial was fitted:

$$\sigma = C_o + C_1\varepsilon_p + C_2\varepsilon_p^2 + C_3\varepsilon_p^3 + C_4\varepsilon_p^4 + C_5\varepsilon_p^5 \quad (8)$$

The values of these coefficients in the plastic strain ranges used are also listed in Table 1. Figure 3 shows the true stress-plastic strain curves given by these polynomials.

6. The Deformation Parameter $2\ln(d_o/d)$

The measure of deformation is required when comparison is made among distributions of stress and strain between different deformation levels, different materials, and different notch geometries, i.e. pitches. The degree of deformation $2\ln(d_o/d)$ of notched cylindrical specimens can be expressed by the magnitude of the deformation at the net section. This is because fracture always occurs at the net section. This measure of deformation is obtained from the assumptions of the uniform deformation in the immediate vicinity of the net section and the volume constancy in this part. The assumption of the volume constancy can be applied only to plastic strain.

The elastic strain component of the axial strain is thus assumed to be negligible compared t the plastic strain component in the immediate vicinity of the net section. This means that the element $A_o \times \delta l_o$ deforms to the element $A \times \delta l$ under the conditions of the volume constancy and the uniaxial stress state, where A_o, A, δl_o, δl are the initial and current areas and the initial and current lengths of the element. The volume constancy, $A_o \times \delta l_o = A \times \delta l$, gives the engineering axial strain of this element e_z

$$e_z + 1 = \frac{\delta l}{\delta l_o} = \frac{A_o}{A} = (d_o/d)^2 \quad (9)$$

The logarithmic axial strain is thus given by

$$\varepsilon_t = \ln(e_z + 1) = \ln(d_o/d)^2 = 2\ln(d_o/d) \quad (10)$$

This obtained variable $2\ln(d_o/d)$ can be a measure of the deformation parameter at the deformation levels where the elastic strain component is much less than the plastic one. It also plays the role of an average axial strain because a uniform deformation or uniaxial stress state is assumed. Moreover, the ratio d_o / d represents the magnitude of the decrease in the net diameter under tensile deformation at any deformation level. This means that $2\ln(d_o/d)$ can be used as a measure of deformation from infinitesimal to large deformation [14-15].

Table 1. Mechanical properties and polynomial coefficient.

Material ν, E [GPa], σ_Y [MPa]	Plastic strain range	C_o	C_1	C_2	C_3	C_4	C_5
Austenitic stainless steel 0.30, 206, 245.9	$\varepsilon_p \le 0.2$	2.459×10^2	4.389×10^3	-3.265×10^4	2.402×10^5	-8.899×10^5	1.258×10^6
	$0.2< \varepsilon_p \le 0.5$	3.789×10^2	1.535×10^3	1.173×10^3	-1.874×10^3	0.0	0.0
Ni-Cr-Mo steel 0.30, 206, 525	$\varepsilon_p \le 0.1$	5.250×10^2	7.644×10^3	-7.377×10^4	2.596×10^5	0.0	0.0
	$0.1<\varepsilon_p$	7.426×10^2	6.945×10^2	-8.143×10	0.0	0.0	0.0

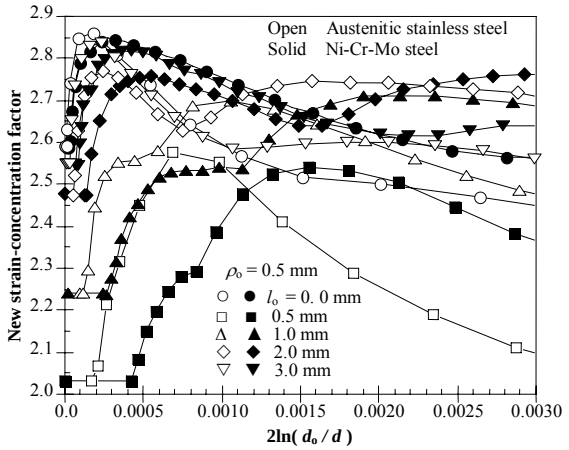

Figure 4. Variations of the new SNCF with deformation for ρ_o = 0.5 mm

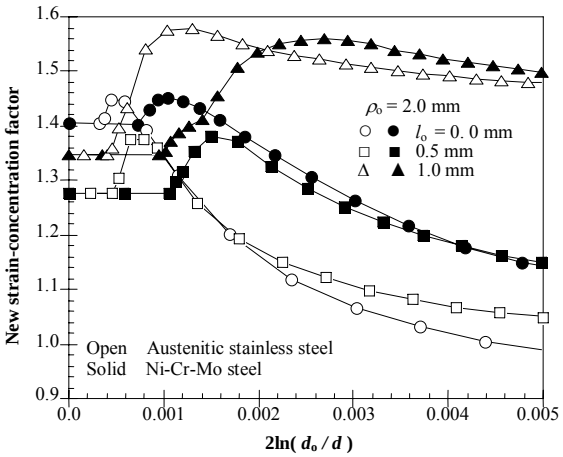

Figure 5. Variations of the new SNCF with deformation for ρ_o = 2.0 mm.

7. Interference Effect on the New SNCF(K_ε^{new})

The variations in the new SNCF K_ε^{new} with $2\ln(d_o/d)$ are given in Figures 4 and 5. The new SNCF is constant inelastic deformation, and the range of $2\ln(d_o/d)$ for this constant value increases with increasing notch radius. It also increases with increasing notch pitch up to $l_o \approx 0.5$ mm. On further increase in the notch pitch, this range decreases and becomes nearly the same as that of the single circumferential U-notch. As plastic deformation develops from the notch root, the new SNCF increases from its elastic value to its maximum, and then decreases on further plastic deformation. Figures 6(a) and (b) show the relation of the elastic K_ε^{new} with half notch pitch l_o and with the ratio (l_o/ L_o). The elastic K_ε^{new} rapidly decreases from its value at l_o = 0.0 mm and reaches its minimum at $l_o \approx 0.5$ mm. On further increase in l_o, the elastic K_ε^{new} gradually increases and finally reaches the value of the circumferential U-notch (l_o = 0.0 mm) at l_o = 5 mm and 2 mm for ρ_o= 0.5 and 2 mm, respectively. Beyond this value of l_o, the elastic K_ε^{new} is nearly constant up to l_o = 25 mm, the maximum half notch pitch in the FEM calculations. The elastic K_ε^{new} in the range $5 \le l_o \le 25$ mm are nearly equal to the elastic K_ε^{new} of the circumferential U-notch. This indicates that the interference effect on the elastic K_ε^{new} is extremely strong in a small range of l_o and nearly vanishes beyond $l_o \approx 5.0$ mm. It should be noted that the same results have been obtained for ρ_o= 2.0mm. However, the interference effects disappears in the range l_o >2.0 mm.

Figure 7 shows the variation of the new average axial strain or new nominal strain $(\varepsilon_z)_{av}^{new}$ and the maximum axial strain $(\varepsilon_z)_{max}$ with deformation. It is clear that the values of $(\varepsilon_z)_{av}^{new}$ and $(\varepsilon_z)_{max}$ for at any level of deformation for l_o = 0.5 mm are less than that for l_o > 0.5mm. Figures 8 and 9 show that the axial strain has concave distribution on the net section for all notch pitches employed. Particularly, the rate of the increase in the axial strain through the net section increases with increasing notch pitch. The axial strain value at the notch root; i.e. the maximum axial strain, increases from it minimum value for l_o = 0.5 mm and reaches maximum value for l_o = 0.0 mm. This indicates that the severe interference effect is more pronounced in the range $0.0 < l_o \le 5.0$ mm.

The tensile load P is calculated using the following equation:

$$P = \int_A \sigma_z \, dA = (\sigma_z)_{av} \, A \tag{11}$$

Where A (= π/4 d^2) is the current net-section area. Therefore, the tensile load P can be related to the deformation parameter $2\ln(d_o/d)$ by

$$P = (\sigma_z)_{av} \, A = \frac{\pi}{4} \frac{d_o^2}{e^{2ln(d_o/d)}} (\sigma_z)_{av} \tag{12}$$

The variation in the tensile load with deformation is shown in Fig. 10. The current results indicate that the rates of increase in the tensile increase with increasing notch pitch. This indicates that the severity of the notch increases with increasing notch pitch. As a result, the single circumferential notch gives more strain concentration than the double circumferential U-notches, especially when the notch pitch is less than 5 mm. This essentially attributed to rate and direction of development of deformation from the notch root. That is, when the double notches are closed to each other, the deformation spreads in inclined direction from the notch root to the pitch center, as shown in Figures

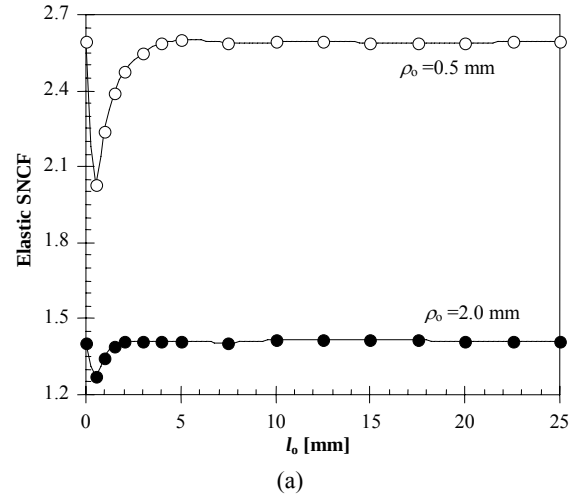

(a)

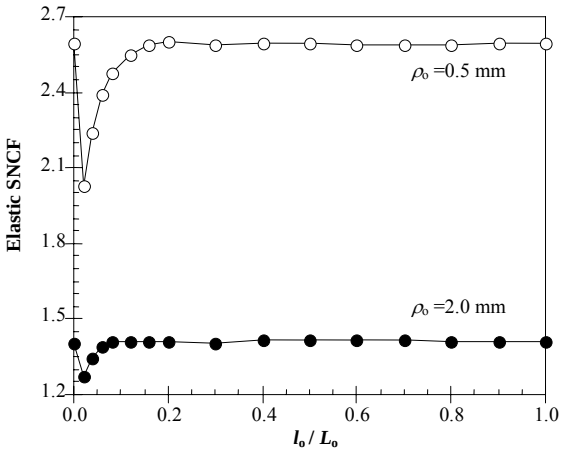

(b)

Figure 6. (**a**) .Variations in elastic new SNCF half notch pitch l_o, **(b)**. Variations in elastic new SNCF with the ratio (l_o/L_o).

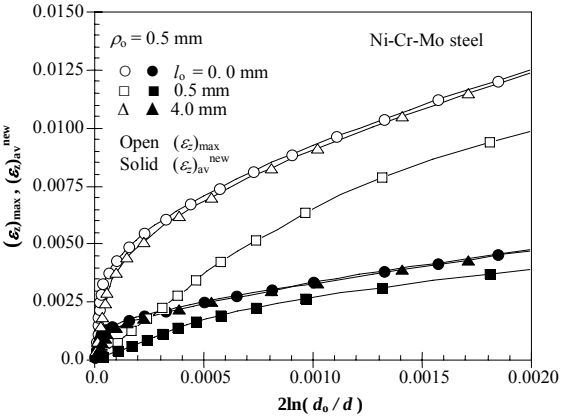

Figure 7. Variations of $(\varepsilon_z)_{max}$ and $(\varepsilon_z)_{av}^{new}$ with deformation.

11, 12 and 13. It is evident from these figures that the severest interference effect occurs when the notch pitch is nearly equal to less than 5 mm. A severe notch is usually understood as a notch having a large strain concentration. This occurs when the deformation is localized at and around the notch tips. This localization of deformation at the notch root is prominent for notch pitches greater than 5 mm; i.e. for notches that can be considered as single circumferential U-notch.

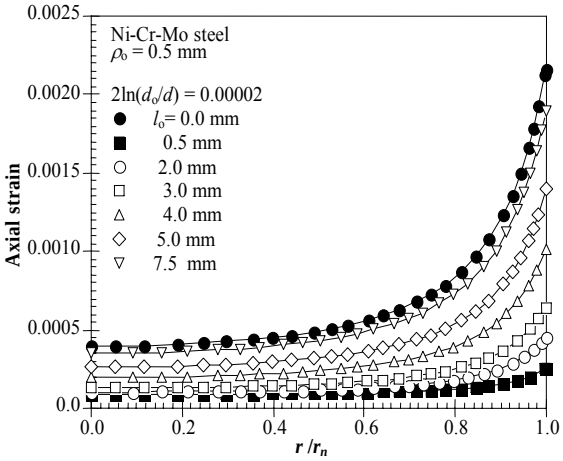

Figure 8. Distributions of the axial strain on the net section for Ni-Cr-Mo steel

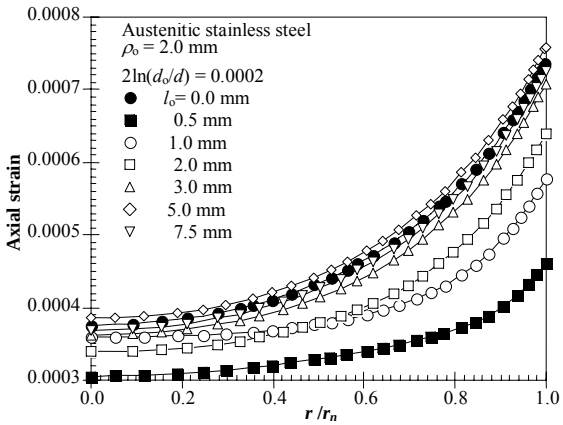

Figure 9. Distributions of the axial strain on the net section for Austenitic stainless steel.

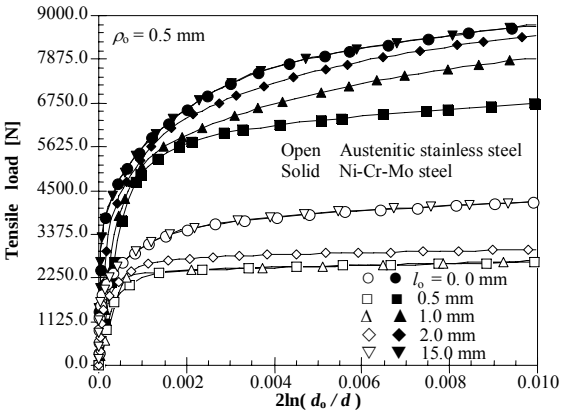

Figure 10. Variations of the tensile load with deformation for ρ_o = 0.5 mm.

It has been proved by the author in previous article that the relations between K_ε^{new} with P/P_Y are independent of the stress – strain curves [29]. Basically, the deformation parameter is related to the tensile load. Therefore, the parameter □; the ratio of deformation parameter to that at yielding at the notch root)is introduced here to eliminate the effect of stress – strain curves.

Figure 14 shows that the relationships of K_ε^{new} versus η are nearly independent of the stress-strain curve.

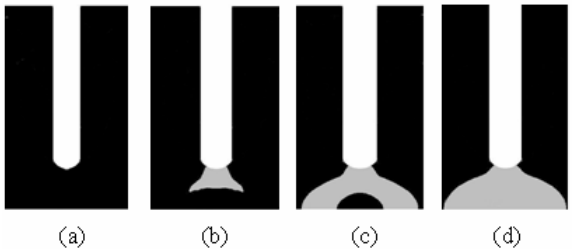

Figure 11. Distributions of axial strain on the net section of a single circumferential U-notch with ρ_o = 0.5 mm, (**a**).Initial yielding at the notch root $2\ln(d_o/d)$ = 0.0000485, (**b**) . $2\ln(d_o/d)$ = 0.000376 , (**c**). $2\ln(d_o/d)$ = 0.000645,(**d**). $2\ln(d_o/d)$ =0.00121 .

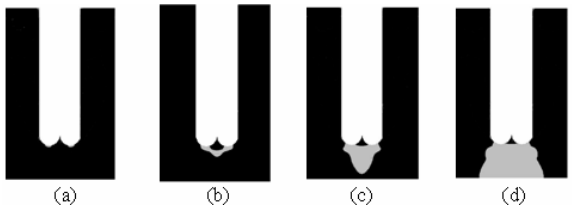

Figure 12. Distributions of axial strain on the net section of double circumferential U-notch with ρ_o = 0.5 mm and l_o = 0.5 mm **(a).** Initial yielding at the notch root $2\ln(d_o/d)$ = 0.00046,

(**b).** $2\ln(d_o/d)$ = 0.00074,(**c).** $2\ln(d_o/d)$ = 0.00181, (**d).** $2\ln(d_o/d)$ = 0.00413.

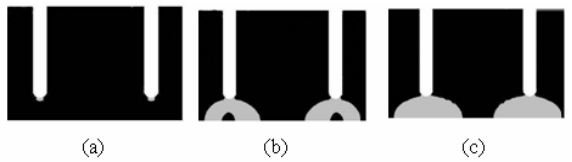

Figure 13. Distributions of axial strain on the net section of a double circumferential U-notch with ρ_o = 0.5 mm and l_o = 4.0 mm **(a)** Initial yielding at the notch root $2\ln(d_o/d)$ = 0.00018274, **(b)** $2\ln(d_o/d)$ = 0.0023982, **(c)** $2\ln(d_o/d)$ = 0.012380.

As a result, the effect of the rate of strain hardening is thus almost negligible on the variation of K_ε^{new} with $2\ln(d_o/d)$. This indicates that the main factor affecting the variation of K_ε^{new} with $2\ln(d_o/d)$ is the magnitude of yield stress. The only factor that affects the shape of K_ε^{new} with η curve is the notch geometry. On the other hand, the stress-strain curves of the ferrous materials used here are very different from each other. This suggests that any ferrous material should have the same variation of K_ε^{new} with η.

8. Conclusions

The interference effect on the new SNCF has been studied for notched cylindrical bars with double circumferential U-notches. The following conclusions can be drawn:

1. The interference effect on the elastic SNCF is prominent in the range $0.0 < l_o < 5.0$ mm for notch radius of 0.5 mm while it is prominent in the range $0.0 < l_o < 2.0$ mm for notch radius of 2.0 mm.
2. The direction of development of deformation from the notch radius is strongly affected by the notch pitch. Particularly, the deformation develops in inclined direction from the notch root to the center of the pitch. On the other hand, the deformation development is symmetric about the center of the net section for single circumferential U-notch (l_o = 0.0 mm) and double circumferential U-notch with $l_o > 5.0$ mm.
3. The new SNCF increases from its elastic value to its maximum as the plastic deformation develops from the notch root. The rate of increase in the new SNCF from its elastic to the maximum value decreases with decreasing notch pitch. The current results indicate that plastic deformation capacity of the notched bars is more pronounced as the notch pitch decreases.

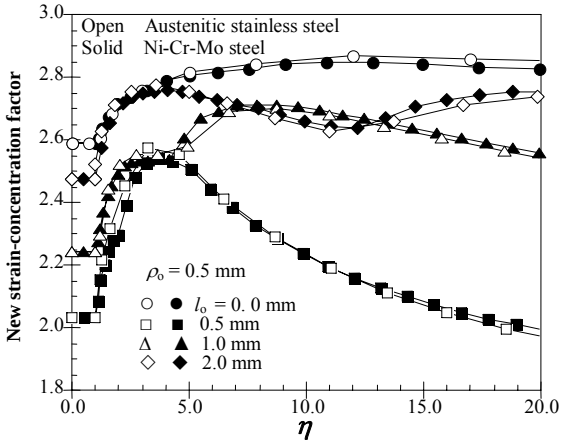

Figure 14. Variation in the new SNCF with non-dimensional parameter η for ρ_o = 0.5 mm.

References

[1] M.M. Leven, M.M. Frocht, "Stress-concentration factors for single notch in flat bar in pure and central bending". J. Appl. Mechanics, Vol. 74, 1952, 560-56.

[2] H.F. Hardrath, L. Ohman, "A study of elastic and plastic stress concentration factors due to notches and fillets in flat plates". National Advisory Committee Aeronautics, NACA Report 1117, 1953.Pilkey W.D. Peterson's stress concentration factors. New York: Wiley; 1997.

[3] Nishida K. Stress concentration. (In Japanese). Tokyo: Morikita Shuppan; 1974.

[4] N.A. Noda, M. Sera, Y. Takase, "Stress concentration factors for round and flat test specimens with notches". Int. J. Fatigue, Vol. 17, No. 3, 1995, 163-178.

[5] A. Kato, "Design equation for stress concentration factors of notched strips and grooved shafts". J. strain analysis, Vol 26, 1991, 21-28.

[6] H. Neuber, "Theory of stress concentration factor for shear-strained prismatical bodies with arbitrary nonlinear stress-strain law". J. Appl. Mechanics, Vol. 28, 1961, 544-550.

[7] P.S. Theocaris, "Experimental solution of elastic-plastic plane stress problems". J. Appl. Mechanics, Vol. 29, 1962, 735-743.

[8] [9] P.S. Theocaris, E. Marketos, "Elastic-plastic strain and stress distribution in notched plates under plane stress". J. Mech. Phys. Solids, Vol. 11, 1963, 411-428.

[9] A. J. Durelli, C.A. Sciammarella, "Elastoplastic stress and strain distribution in a finite plate with a circular hole subjected to unidimensional load". J. Appl. Mechanics, Vol. 30, 1963,115-121.

[10] P.S. Theocaris, "The effect of plasticity on the stress-distribution of thin notched plates in tension". J. Franklin Inst., Vol. 279, 1965, 22-38.

[11] K. Ogura, N. Miki, K. Ohji, "Finite element analysis of elastic-plastic stress and strain concentration factors under plane strain and axisymmetric conditions". (In Japanese).Trans. Japan Soc. Mech. Engrs., Vol. 47, 1981, 55-62.

[12] S.J. Hardy, M.K. Pipelzadeh, "An assessment of the notch stress-strain conversion rules for short flat bars with projections subjected to axial and shear loading". J. Strain Analysis, Vol. 31, No. 2, 1996, 91-110.

[13] T. Majima, "Strain-concentration factor of circumferentially notched cylindrical bars under static tension". J. Strain Analysis, Vol. 34, No. 5, 1999, 347-360.

[14] H.M Tlilan, S. Yousuke, T. Majima, "Effect of notch depth on strain-concentration factor of notched cylindrical bars under static tension". European Journal of Mechanics A / Solids, Vol. 24, No. 3, 2005, 406-416.

[15] W.N.Jr. Sharp, M. Ward, "Benchmark cyclic plastic notch strain measurements". Trans. ASME, J. Engg Mater. Technol., Vol. 105, 1983, 235-241.

[16] A.R. Gowhari-anaraki, S.J. Hardy, "Low cycle fatigue life predictions for hollow tubes with axially loaded axisymmetric internal projections". J. Strain Analysis, Vol. 26, 1991, 133-146.

[17] W.N.Jr. Sharp, "ASME 1993 Nadai Lecture-Elastoplastic stress and strain concentrations". Trans. ASME, J. Engng Mater. Technol., Vol. 117, 1995, 1-7.

[18] Z. Zeng, A. Fatemi, "Elasto-plastic stress and strain behaviour at notch roots under monotonic and cyclic loadings". J. Strain Analysis, Vol. 36, 2001, 287-288.

[19] G. Harkegard, T. Mann, "Neuber prediction of elastic-plastic strain concentration in notched tensile specimens under large-scale yielding". J. Strain Analysis, Vol. 38, 2003, 79-94.

[20] P. Livieri, G. Nicoletto, "Elastoplastic strain concentration factors in finite thickness plates". J. Strain Analysis, Vol. 38, 2003, 31-36.

[21] G. Glinka, "Energy density approach to calculation of inelastic strain-stress near notches and cracks". Engng. Fracture Mechanics, Vol. 22, 1985, 485-508.

[22] [23] Fuchs, H.O., Stephens, R.L. Metal Fatigue in Engineering. New York: John Wiley and Sons; 1980.

[23] [24] H.M. Tlilan, N. Sakai, T. Majima, "Strain-concentration factor of a single-edge notch under pure bending. (In Japanese)". Yamanashi District Conference, No. 40-4, Japan, October 10th 2004.

[24] H.M. Tlilan, N. Sakai, T. Majima, "Strain-concentration factor of rectangular bars with a single-edge notch under pure bending, (In Japanese)". J. Soc. Mat. Science, Vol. 54, No. 7, 2005, 724-729.

[25] [26] H.M. Tlilan, N. Sakai, T. Majima, "Effect of notch depth on strain-concentration factor of rectangular bars with a single-edge notch under pure bending". Int. J. Solids and Structures, Vol. 43, 2006, 459–474.

[26] T. Majima, "Interference effect of notches (1st report, evaluation of interference effect of notches on yield point load of double U-shaped notches by upper and lower bound theorems)". Trans. Japan Soc. Mech. Engrs., Vol. 48, No. 430, 1982, 719-728.

[27] T. Majima, K. Watanabe, "Interference effect of notches (2nd report, an experimental investigation of interference effect on strength and deformation properties of notched bars with double symmetrical u-notches". Trans. Japan Soc. Mech. Engrs., Vol. 48. No.433, 1982, 1186-1194.

[28] H.M. Tlilan, A.S. Al-Shyyab, A.M. Jawarneh, A.K. Ababneh, "Strain-concentration factor of circumferentially v-notched cylindrical bars under static tension". Journal of Mechanics, Vol. 24, No. 4, 2008, 419-428.